International Journal of Phytoremediation

ISSN: 1522-6514 (Print) 1549-7879 (Online) Journal homepage: www.tandfonline.com/journals/bijp20

Adsorption of crystal violet dye using *Embelia schimperi* biochar: optimization using response surface methodology

Margaret Chepkemoi Koske, Michael David Otieno , Ismael Okoth Oduor & Charity Mutile Muendo

To cite this article: Margaret Chepkemoi Koske, Michael David Otieno , Ismael Okoth Oduor & Charity Mutile Muendo (05 Aug 2026): Adsorption of crystal violet dye using *Embelia schimperi* biochar: optimization using response surface methodology, International Journal of Phytoremediation, DOI: 10.1080/15226514.2026.2711109

To link to this article: https://doi.org/10.1080/15226514.2026.2711109

Published online: 05 Aug 2026.

Submit your article to this journal

Article views: 51

View related articles

View Crossmark data

Full Terms & Conditions of access and use can be found at
https://www.tandfonline.com/action/journalInformation?journalCode=bijp20

INTERNATIONAL JOURNAL OF PHYTOREMEDIATION
https://doi.org/10.1080/15226514.2026.2711109

Taylor & Francis
by informa

Check for updates

Adsorption of crystal violet dye using *Embelia schimperi* biochar: optimization using response surface methodology

Margaret Chepkemoi Koske[a], Michael David Otieno[b], Ismael Okoth Oduor[c], and Charity Mutile Muendo[a]

[a]Department of Science and Technology, Koitaleel Samoei University College; [b]Department of Sport Science, Koitaleel Samoei University College; [c]Department of Finance and Accounting, Koitaleel Samoei University College

ABSTRACT

Crystal violet (CV) is a highly soluble dye used extensively in the textile industry and healthcare. The environmental complex structures of CV result in destructive effects on humans, animals, and the environment. In this study, adsorption of CV using *Embelia schimperi* biochar as an adsorbent was investigated. *E. schimperi* waste has unique structural properties and can be used as a biochar and utilized as a low-cost adsorbent. The experiments were two-tier designed: both the classical and optimization by response surface methodology (RSM). Three parameters were evaluated, which are adsorbent dosage, contact time, and pH, while the responses in this study are CV removal (%). Optimization studies were performed using RSM central composite *Design* using Minitab 17. A quadratic model was chosen for the response. The correlation coefficient, R^2, for the quadratic model of CV removal (%) was 0.98, and the $p < 0.0001$. The optimum CV removal (%) predicted was found at 98%, by using 0.11 g of adsorbent dosage, 60 min of contact time, and pH of 7.5 at desirability of 1.0. It was concluded that the spent *E. schimperi* biochar can be used as an effective adsorbent for CV removal from aqueous solution.

KEYWORDS

Embelia schimperi waste; biochar; adsorption; crystal violet; response surface methodology

Introduction

The toxic effluents generated by the industrial and agricultural sectors through large quantities of wastewater are enormous (Chowdhary *et al.* 2020; Kumari *et al.* 2025). The major sources with significant pollution contribution are the textile industry, known to emit discharges in form of wastewaters with significant kinds of toxic untreated synthetic dyes (Periyasamy 2024). During the process of dyeing, approximately 10–25% are discharged as waste effluents into the environment. Crystal violet (CV), a triphenylmethane cation dye, is widely used and poses a high risk to the water environment and has caused enormous concern. CV is quite toxic and classified as carcinogenic (Qi *et al.* 2021).

CV has low biodegradability (Lin *et al.* 2021). Its presence in even an insignificant low concentration of 1 mg/L reduces penetration of light on the surface, affecting the photosynthesis of aquatic plants (Amin *et al.* 2021). Therefore, it is necessary to remove CV dye from wastewater before allowing it into aquatic environments (Foroutan *et al.* 2021). Several methods of removal of waste, including chemical, biological, and physical methods, have been employed (Kumari *et al.* 2024). Scientists have found different methods to effectively remove various kinds of cationic dyes. These methods include membrane separation and cation exchange resins (Mustafanejad *et al.* 2021; Omokpariola 2021). The reverse osmosis (Khalil *et al.* 2021), micellar enhanced ultrafiltration (Verma and Sarkar 2020). Others include combined biological–chemical degradation (Aamir *et al.* 2021). Separation techniques have also been established; among these are coagulation separation methods (Samrot *et al.* 2021); photodegradation methods have basically been found to be effective according to Ahmad *et al.* (2021): chemical oxidation (Rehman *et al.* 2018), conventional water treatment (Berk *et al.* 2025), electrocoagulation, and adsorption (Vidya Vijay *et al.* 2019; Chahinez *et al.* 2020; Ganea *et al.* 2021).

The most recent advances for the removal of textile dyes have employed the adsorption method (Sackey *et al.* 2021; Vigneshwaran *et al.* 2021; Tripathi *et al.* 2022; Sarioz *et al.* 2024). These have involved the use of biochar and activated carbon and they have been found to have excellent adsorbent properties for both organic and inorganic pollutants (Cheng *et al.* 2021; Othmani *et al.* 2021). The biochars are low cost (Srivatsav *et al.* 2020) and they possess remarkable textural and physical properties such as high pore volume, specific surface area, good chemical stability, and rigidity (Li *et al.* 2020; Wang *et al.* 2021). They are useful in water purification (Hu *et al.* 2019; Palansooriya *et al.* 2020; Wang *et al.* 2021). Studies by several researchers reveals development of various lignocellulosic derived wastes biochar applied to water decolourization (Akdemir *et al.* 2023) examples of such biomass from wood sources

CONTACT Margaret Chepkemoi Koske margaret@ksu.ac.ke Department of Science and Technology, Koitaleel Samoei University College.
© 2026 Taylor & Francis Group, LLC

(Rangabhashiyam and Balasubramanian 2019), fruit peels (Bing Zhang *et al.* 2020), macro-algae, (Gurav *et al.* 2021) orange peel, coconut shells, golden shower pods (Tran *et al.* 2017) and roots (Isik *et al.* 2023). An increasing number of research shows that most biochar modified to increase its adsorption capacity. However, the modified biochar raises the associated expenses and may result in waste and contamination from the chemical reagents. Finding an unmodified biochar with a high adsorption capability toward wastewater is therefore essential. Selecting the right feedstock is essential for the creation of an effective biochar since prior research has shown that the raw materials have a significant impact on the physicochemical characteristics and adsorption capacity of biochar.

In this study, used *Embelia schimperi* was identified for investigation of its suitability as a biosorbent, after studies revealed it contains embelin, a useful precursor in semi-synthetic reactions (Koske *et al.* 2022). However, it generates waste, and in this current study, its residue was selected for evaluation as a low-cost precursor for the preparation of a potential adsorbent and used as an alternative green adsorbent for the first time to explore the removal process of cationic dye (CV) from aqueous media without modification. Three parameters are adsorbent dosage (0.2 – 1.2 g), contact time (30–240 min), and pH (2–12), while the responses are the percentage of CV removal. The adsorption performance of CV removal was studied using the classical method and response surface methodology (RSM). Analysis of variance (ANOVA) was also used to justify the adequacy of the models for CV removal (%). The interaction effect of parameters using three-dimensional (3D) response surface graphs and diagnostic plots for predicted versus actual values of experimental responses were also examined to study the residual errors.

Methodology

Chemical reagents

The CV ($C_{25}H_{30}N_3Cl$, M.W 407.99 g/mol, 88% purity, sodium hydroxide (97% purity), and hydrochloric acid (37% purity) were purchased from Loba Chemie Pvt., Ltd, India. All the chemicals were used as they are without further purification.

Preparation of E. schimperi biochar

The dry *E. schimperi* stem bark residue was used to prepare the adsorbent. This biochar was prepared by the pyrolysis method, which proceeded under oxygen-free conditions. The obtained biomass was covered with aluminum foil and pyrolyzed at 500°C in a muffle furnace (ELF11/14B 220–240 V 1 PH + N) model. The heating rate was adjusted to 5°C/min for 4 h to attain a slow pyrolysis process until the maximum temperature was obtained. The produced biochar was sieved and stored in airtight sample bottles, kept in a desiccator, and used for further analysis. Functional group analysis of the biochar before and after adsorption was carried out using OMNIC version 9.1.24 software; ATR-FTIR spectra were captured on a Nicolet 6700 (Thermo Scientific, USA) spectrometer (Thermo Fisher Scientific), and the surface characterization was evaluated using scanning electron microscopy (SEM) and tunneling electron microscopy (TEM) using JEOL JSM 6390.

Batch adsorption studies

A stock solution of CV (1000 mg/L) was prepared using distilled water and the working standards were prepared from successive dilution of the stock solution. Batch adsorption studies, the constant parameters in this study were determined, namely; initial concentration (2 mg/L), temperature (30 °C), agitation speed of orbital shaker (60 rpm) and volume of CV solution (40 mL), this finding was in agreement with studies carried out by Singh *et al.* (2011) consequently, the optimum agitation speed from preliminary study was at 60 rpm.

The necessary adsorbent dose was weighed and transferred to the Erlenmeyer flasks, shaken at a constant temperature of 30°*C* in an incubation shaker at 60 rpm. When time of operation was complete, the supernatant and the spent adsorbent were separated by filtration. The residual dye concentration in the supernatant was analyzed by measuring the solution absorbance at λ = 584 nm using a UV–visible spectrophotometer (Model - Beckham Coulter DU 720). All experiments were conducted in triplicate and the average values were taken. The percentage of CV removal calculated using Equation (1). The data were inserted in Minitab software (17) for analysis

Percentage of CV removal was given by

$$Y\% = \left(\frac{C_O - C_f}{C_O} \times 100\% \right) \tag{1}$$

where C_o is the initial dye concentration and C_f is the final dye concentration of CV.

Classical experiments

In order to investigate the adsorption effect caused by the parameters accurately, few constant variables were determined in a preliminary study, which are temperature (30 °C), agitation speed (60 rpm), initial concentration of CV (2 mg/L), and volume of CV solution (40 mL). The classical adsorption experiments were run by varying one factor while holding the others at a specified value. The adsorption parameters namely adsorbent dose (0.2, 0.4, 0.6, 0.8, 1.0, and 1.2 g), time (60, 120, 200, and 400 min), and pH (2, 4, 6, 8, 10, and 12) effect on the CV removal efficiency were investigated.

Experimental design and RSM

The setting of CCD was in Minitab 17 software, the independent variables were *A* (pH), *B* (contact time), and *C* (adsorbent dose), while the response variable was % (CV dye removal). The detailed information of each parameter with its minimum (low) level and maximum (high) which are shown in Table 1.

From the design of experiment, the total number of runs carried out was 20 with different operating conditions. The regression model of experimental data was determined using an empirical polynomial equation; the statistical significance of the model and the regression term evaluations were based on ANOVA.

Optimization studies

Comparisons between the actual experimental data and the predicted experimental results using Minitab 17 were evaluated. The analysis from the experimental data embedded on an experimental response, which was percentage of CV removal. The response then underwent a set of evaluations involving ANOVA, the polynomial regression model equation developed, and diagnostic plot for predicted values versus actual values; 3D surface plot revealed the existence of the behavior of the model generated by Minitab 17 software.

Table 1. Real variables and the respective coded values.

Coded variable	Level	−1.633	−1	0	1	+1.633
Real variables	pH (*C*)	5.05	6	7.5	9	9.95
	Time (*B*) (min)	11.01	30	60	90	108.99
	Ads dose (*A*)	0.01	0.02	0.11	0.2	0.26

Table 2. Statistical analysis of removal of % CV with respect to pH.

S/no	pH	% CV removal
1	2	60 ± 1.73
2	4	62 ± 2.51
3	6	83 ± 2.08
4	8	81 ± 2.07
5	10	81 ± 3.05

Results and discussion

Classical experiments

Effect of the pH

Table 2 and Figure 1 show the statistics and the effect of pH on the CV removal. In fact, a preliminary study on the effect of pH on CV removal was carried out at a range of pH 2 to pH 10. In summary, the percentage of CV removal was between 60% and 70%; it was low and inefficient at the acidic range of pH 2–5. This could be due to the availability of an excess amount of Hydrogen ions, which protonated the functional group of the adsorbent. The protonation caused the adsorption to become more positive, developing a repulsive force which caused the positively charged CV molecules to be adsorbed on the adsorbent. At pH 2, CV removal was the lowest compared to pH 6. (Pal and Sheetal 2024). The percentage CV removal steadily increased to 85%; this was the equilibration state theoretically, CV is a cationic dye, and it exists in the positively charged ionic state in solution. The effectiveness of cationic dye trapped on an adsorbent surface purely depends on the surface charge density of the adsorbent, which is consequently influenced by the pH solution (Zhang *et al.* 2018). Beyond the pH 10, the negatively nature charge density of the adsorbent causes deprotonation of functional group of the adsorbent. Hence, the positive charged CV ions efficiently adsorbed to the negatively charged adsorbent surface due to an increase in the electrostatic force of attraction (Muthukumaran *et al.* 2016).

Effect of contact time. Table 3 and Figure 2 show the effect of time on % CV removal. A significant increase in the percentage of CV removal from 60% to 90% is observed

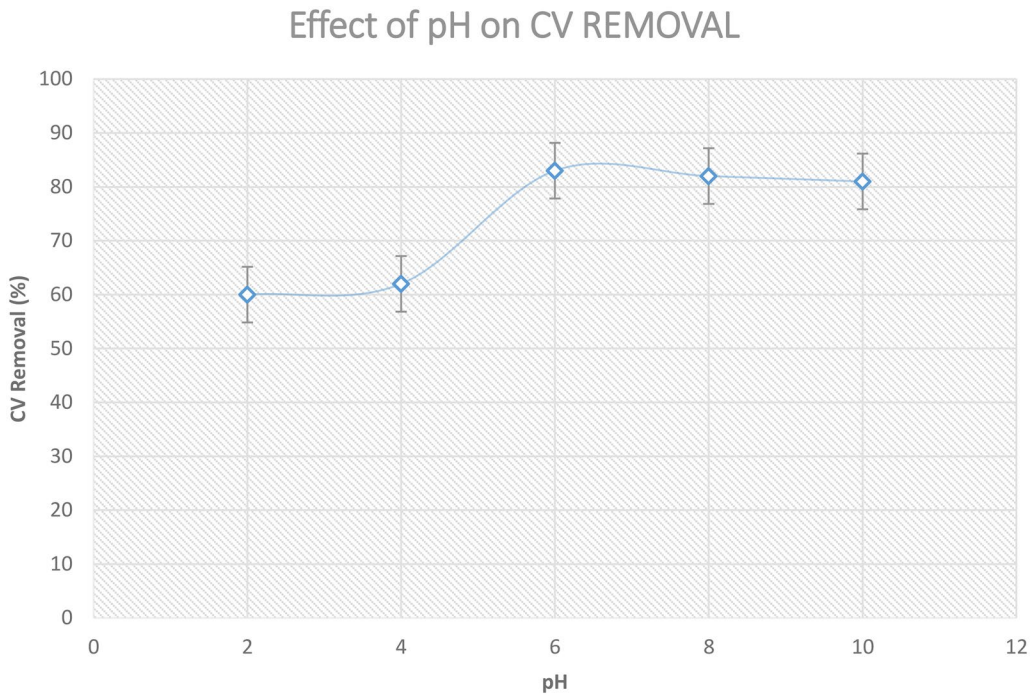


Figure 1. Removal of CV with relation to p00H.

with the increase of contact time from 60 to 90 min, respectively. The CV removals (%) continue to show an increasing trend with a maximum at 98%, which occurred at 60 min of contact time. The increased dye adsorption can be related to the availability of a large number of active adsorption sites available at the outer surface as well as inner pores of the adsorbent particles (Nono *et al.* 2025).

Table 3. Statistical analysis of removal of % CV with respect to time (min).

S/no	Time (min)	% CV removal
1	40	38 ± 2.01
2	60	98 ± 2.08
3	100	83 ± 2.08
4	180	80 ± 1.52
5	250	76 ± 2.64

Effect of adsorbent dosage. The relationship between the % CV removal and adsorbent dose is shown in Figure 3 and Table 4. According to the results obtained, the percentage removal of CV showed a steady decrease from 78% to 74% with increased % CV removal at lower adsorbent dose dosage of 0.1 and 1.1 g. This is possible due to the available

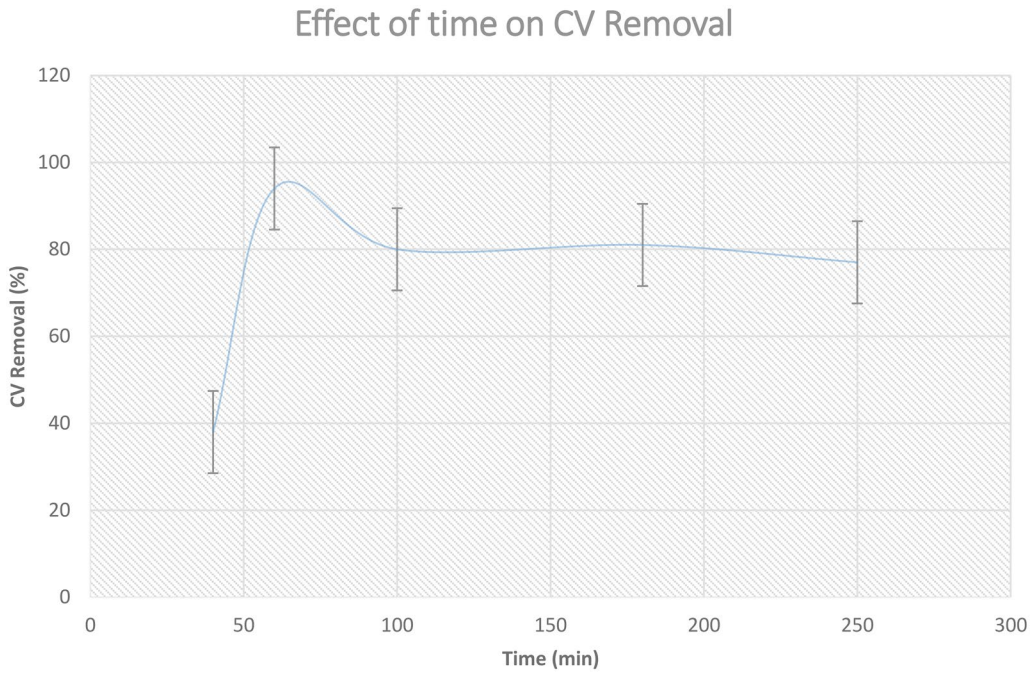


Figure 2. Removal of CV with variation in time.

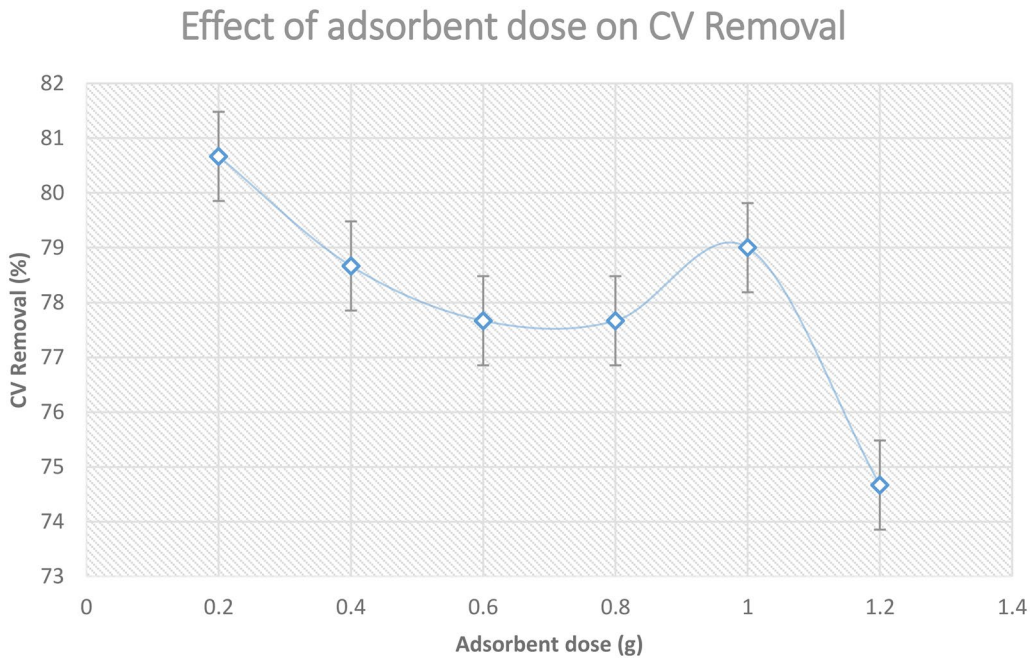


Figure 3. Removal of CV with variation in adsorbent dosage.

increased adsorption sites (Kumar *et al.* 2019).

RSM

In this study, 20 experiments were generated as per the design of experiment in combination with specified parameters using statistical experimental design (RSM—Minitab 17). This was done to determine the synergistic effects as well as the singular effect of the variables toward the efficiency of CV removal. Table 5 shows the experimental design and the response value. The maximum percentage of CV removal was 98.5% with the operating conditions of 0.11 g of adsorbent dosage (*A*), 60 min of contact time (*B*), and pH 7.5 (*C*); several types of models, namely, linear, 2FI, quadratic, and cubic models, were investigated. The design recommended a quadratic model for CV removal (%) with R^2 0.9426 and adjusted R^2 0.8788 as shown in Table 7.

The RSM generated a polynomial regression model with coded factors reflecting the interaction and significance of variables toward efficiency of CV removal. The empirical formula for polynomial regression model in terms of coded parameters studied for CV removal (%) Equation (2) is modeled according to data in coded variables generated by Minitab 17 software.

$$\%\mathrm{CV} = 97.8 + 3.62A + 9.03B - 2.69C - 5.15A^2 - 6.18B^2 - 3.73C^2 - 0.99A \times B + 2.01A \times C - 3.26B \times C \quad (2)$$

From the model, the observed positive sign in the coded Equation (2) indicates that CV removal increases with the increase of the respective parameters. This figure shows the relationship between actual and predicted values of responses for CV removal by *E. schimperi* biochar. The *F*-test ANOVA was used to test the statistical significance of the model; whereas *p*-value was used to check the significance and pattern of interaction between the experimental parameters shown in Table 6. If the value of p-value was less than 0.05 (95% confidence level), the model terms are considered statistically significant (Lu *et al.* 2023). In contrast, values greater than .10 are considered statistically insignificant (van Rijn *et al.* 2017).

From Table 6, the Model *F*-value was 14.77 and the *p*-value was <.0001. For the CV removal (%), the following terms were significant with *p*-value less than .05: pH (*A*), contact time (*B*), adsorbent dosage (*C*), the interactive effect between pH and contact time (*AB*), squared effect of contact time (A^2), contact time (B^2), and adsorbent dose (C^2). The model summary in Table 7 shows R^2 0.9426 and R^2 adjusted 0.8788.

In these results, the squared term for contact time, pH, adsorbent dose, and the interaction between pH and time are significant at the α= 0.05 significance level.

Contour plots

The contour curves are displayed in Figure 4a–c because of the model terms that are quadratic and are statistically significant. The highest values of rating for adsorbent dose are displayed in the darker region of the plot, corresponding to high values of both adsorbent dose and contact time while holding the pH constant at 7.5. In Figure 4b, the time is held at 60, and in Figure 4c, the adsorbent dose is held at 0.11 g.

The interaction plots for percentage CV between two variables, that is pH, time × pH, and adsorbent dose × time illustrated in Figure 5, are all curvatures and not linear. These supported the choice of quadratic model.

Table 4. Statistical analysis of removal of % CV with respect to adsorbent dose (g).

S/no	Adsorbent dose (g)	% CV removal
1	0.2	81 ± 0.57
2	0.4	78 ± 1.53
3	0.6	77.8 ± 0.57
4	0.8	77.6 ± 1.52
5	1	79 ± 1.6
6	1.2	74.6 ± 1.6

Table 5. Experimental design matrix and response values.

Run	pH (*A*)	Contact time, min (*B*)	Run adsorbent dosage, g (*C*)	Removal of CV (%)
1.	0.000	1.633	0.000	96.1
2.	0.000	−1.633	0.000	64
3.	0.000	0.000	−1.633	76
4.	−1.633	0.000	0.000	97.6
5.	0.000	0.000	0.000	98.1
6.	0.000	0.000	1.633	92
7.	0.000	0.000	0.000	97.9
8.	1.633	0.000	0.000	78
9.	1.000	1.000	1.000	96.1
10.	1.000	1.000	−1.000	91
11.	1.000	−1.000	1.000	78
12.	0.000	0.000	0.000	98.3
13.	0.000	0.000	0.000	96.9
14.	−1.000	1.000	1.000	89
15.	−1.000	1.000	1.000	79
16.	−1.000	−1.000	−1.000	78
17.	0.000	0.000	0.000	97.5
18.	0.000	0.000	0.000	98.5
19.	−1.000	1.000	−1.000	87
20.	1.000	−1.000	−1.000	67

Table 6. ANOVA.

Source	DF	Adj SS	Adj MS	*F*-value	*p*-value
Model	10	2402.02	240.20	14.77	<.0001
Blocks	1	0.00	0.00	0.00	.991
Linear	3	1359.05	453.02	27.86	.000
pH	1	96.7	96.70	5.95	.037
Time	1	1087.9	1087.90	66.91	.000
Ads dose	1	174.44	174.44	10.73	.010
Square	3	917.62	305.87	18.81	.000
pH × pH	1	183.58	183.58	11.29	.008
Time × time	1	505.14	505.14	31.07	.000
Ads dose × ads dose	1	350.73	350.73	21.57	.001
Two-way interaction	3	125.35	41.78	2.57	.119
pH × time	1	85.15	85.15	5.24	.048
pH × ads dose	1	32.40	32.40	1.99	.192
Time × ads dose	1	7.80	7.80	0.48	.506
Error	9	146.33	16.26		
Lack of fit	5	145.11	29.02	95.15	.000
Pure error	4	1.22	0.30		

Table 7. Model summary.

S	R^2	R^2 (adj)
4.03220	94.26%	87.88%

Table 8. Comparison of crystal violet adsorption by several other adsorbents.

Adsorbent	Contact time	Temperature	Initial dye conc	Adsorbent dosage in g	pH	Adsorption capacity	Removal efficiency (%)	References
Rice husk biochar	24 h				8	24.45 mg/g		Homagai *et al.* (2022)
Sugarcane bagasse		20	40.1 mg/L	0.4 mg	5	5 mg/L	97.46	Kumari *et al.* (2024)
Modified acacia leaves					6	299.70	96.4	Essekri *et al.* (2023)
Agricultural waste		338 K	10 mg/L	20 mg	11	99.50 mg/g	98	Moharm *et al.* (2022)
Rice husk magnetic nanocomposite	120 min				7.	185.6 mg/g		Luyen *et al.* (2020)
Magnetic chitosan nanocomposite	140 min	25 °C	77 mg/L	1 g		–	72	Massoudinejad *et al.* (2019)
Natural zeolite					10	177.75 mg/g		Sarabadan *et al.* (2019)
Iron-based metal organic framework			5 mg/L	0.1	6	26.65 mg/g.	100	Soni *et al.* (2020)
Orange peel polyvinyl/caraagean	160 min	25 °C		0.05 g			89	Radoor *et al.* (2025)
Hyacinth	120 min		500 ppm		7.8	322.58 mg/g	99.36	Kulkarni *et al.* (2017)
Banana peel				0.1 g	7	94 mg/g	97	Sayed *et al.* (2025)
sugarcane bagasse (alkaline)	30 min	25 °C	40 mg/L	50 mg		107.5 mg/g	96.35	El Naeem *et al.* (2022)
E. schimperi biochar	60 min				7.5	0.11 g	98	Current study

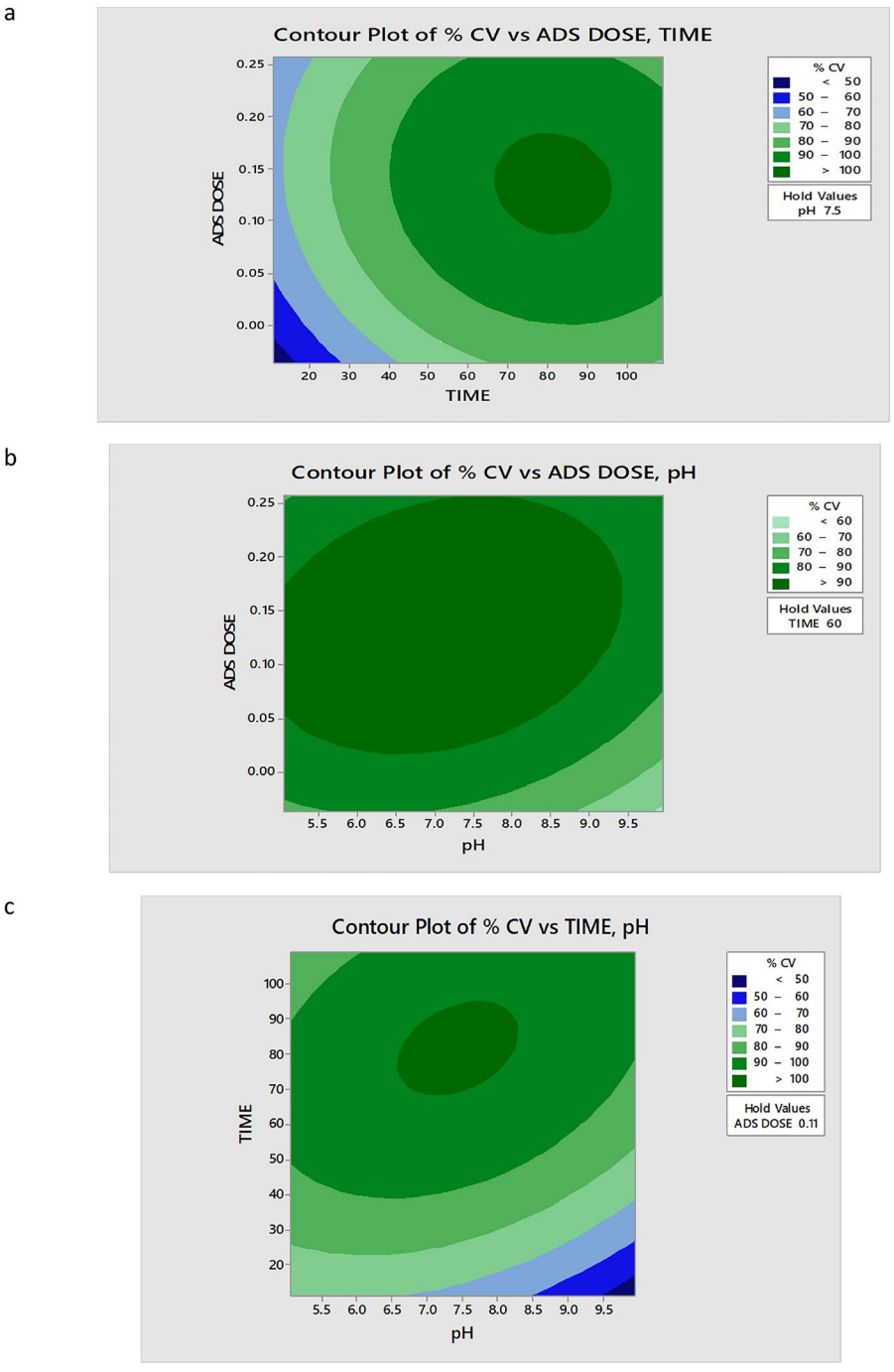


Figure 4. Contour plot for % CV versus ads dosage, time (a). % CV versus ads dosage, pH (b). % CV versus ads pH, time (c).

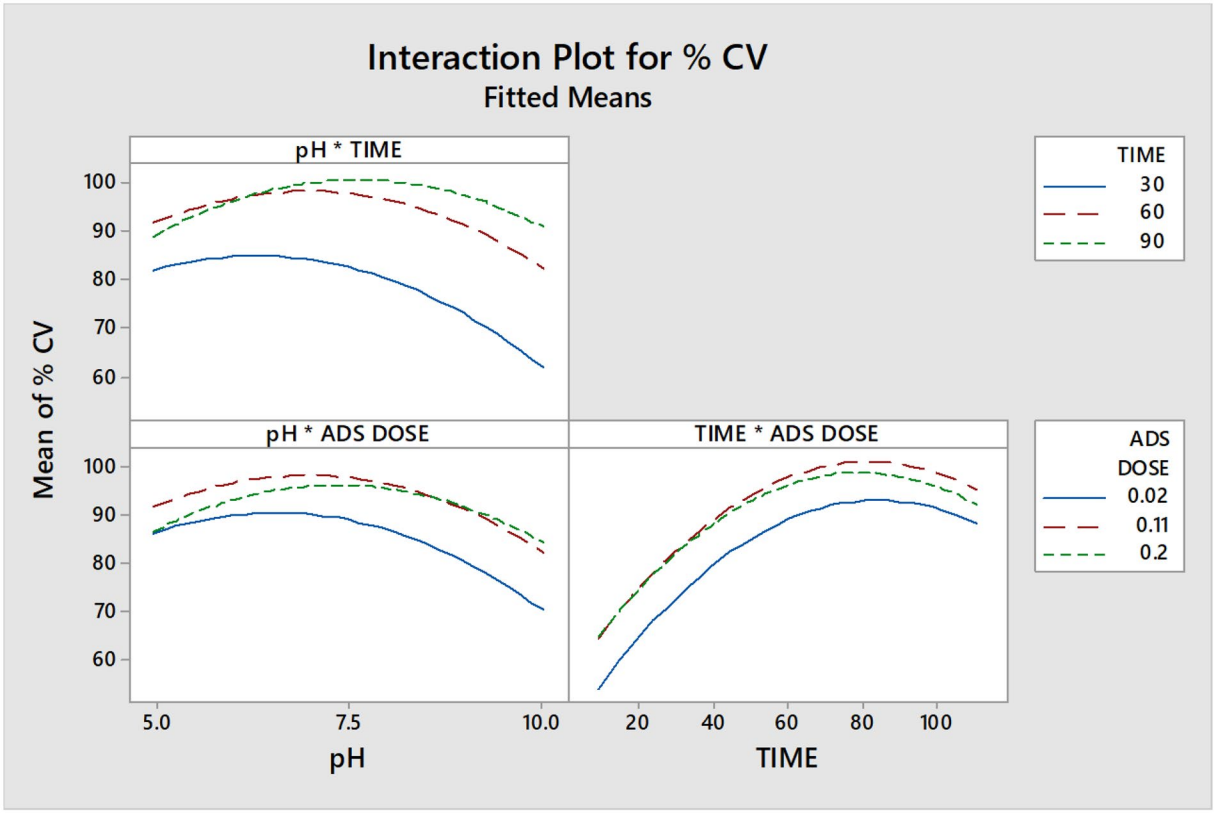


Figure 5. Plots showing interaction plots for percentage CV (%).

3D response surface graphs captured in Figures 6d–f display the effect of the potential relationship between the variables on the CV dye removal while holding other variables constant. The graph in Figure 6d indicates that by increasing the adsorbent dosage or contact time and using pH at 7.5, the CV removal (%) will increase. Meanwhile, Figure 6e shows that increasing pH and contact time and using adsorbent dosage at 0.11 will increase the CV (%) removal, and Figure 6f shows the effect of adsorbent dose and pH. These results resonate with the classical experiment, study for the effect of adsorbent dosage, contact time, and pH on CV removal (%).

Process optimization validation

From the optimization of desirability function generated by Minitab (Ver. 17), the best optimization point for CV removal (%) was picked accordingly on the highest desirability function. The optimum values of process variables for CV removal were obtained using adsorbent dosage 0.11 g, contact time 60 min, and pH of 7.5, resulting in 98% of CV dye removal. These selected conditions were within the experimental design proposed by the software. A validation experiment was carried out in the laboratory using the above optimal conditions, and the percent response was 98%.

The adsorption capacity of different adsorbents on CV is shown in Table 8, and similar observations to our study at a pH of 6 were made using modified acacia leaves by Essekri *et al.* (2023) and rice husk magnetic nanocomposite by Luyen *et al.* (2020)

FTIR characterization

The FTIR spectra of *E. schimperi* biochar Figure 7g before adsorption exhibited characteristic absorption bands at approximately 3304.79 cm^{-1} (O–H stretching), 2924.68 cm^{-1} (aliphatic C–H stretching), 1707.73 cm^{-1} carbonyl peaks, 1637.01 cm^{-1} (aromatic C=C stretching), and 1050 cm^{-1} (C–O stretching). After adsorption, Figure 7h shows these bands shifted to lower wavenumbers and showed reduced intensity. The O–H band shifted to 3257.64 cm^{-1}, while the aromatic C=C band moved to 2921.68 cm^{-1}. The carbonyl peak has disappeared; similarly, the C–O stretching vibration shifted to 1030 cm^{-1}. These observed changes suggest that the hydroxyl, carboxyl, and aromatic functional groups actively participated in the adsorption process through hydrogen bonding, electrostatic attraction, surface complexation, and π–π interactions. The appearance of additional bands in the lower wavenumber region further confirms successful adsorption of the CV onto the biochar surface.

SEM/TEM characterization

SEM and TEM of the *E. schimperi* biochar before adsorption were performed using JEOL JSM 6390. The surface constitution is critical for biochar reactivity, and the magnification images of the biochar shown in Figure 8j,k show that the surface was smooth and irregular in Figure 8i. Figure 8j reveals a surface of prepared layered and porous structure due to the intrinsic nature of the biochar. TEM images observed in Figure 8k reveal an irregular surface with different shapes and many flakes, and the surface became

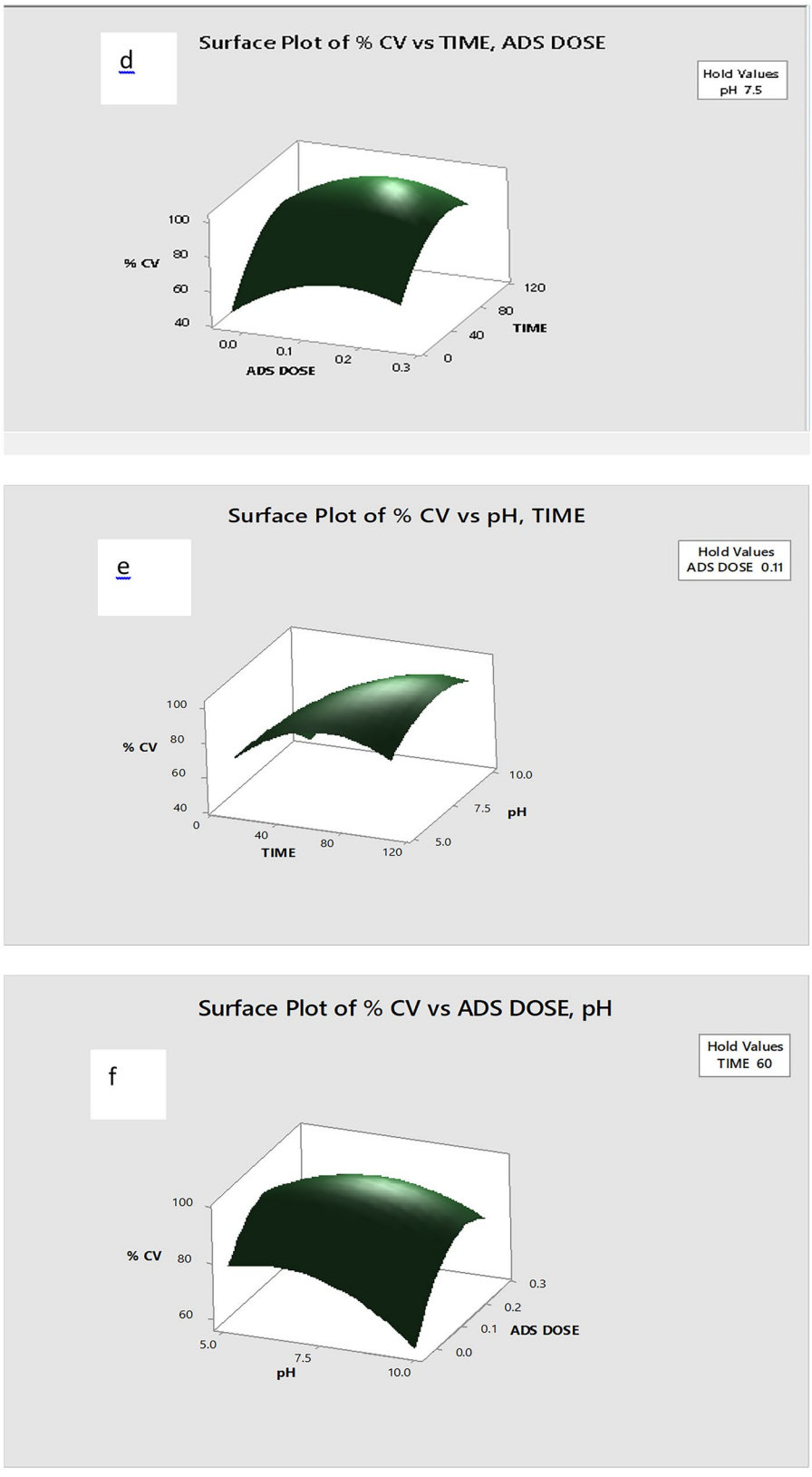


Figure 6. 3D plots: (d) the effect of pH and adsorbent dosage, (e) the effect of pH and time, and (f) the effect of adsorbent dosage and pH on the CV removal (%).

much rougher and more heterogeneous, attributed to the enhancement of superficial area. Compared with l, the surfaces of ESB in Figure 8l had noticeable metal luster, indicating that the adsorbed CV assembled on the surface of biochar.

Conclusion

In this study, *E. schimperi* biochar served as an effective low-cost adsorbent in the removal of CV from aqueous solutions. Adsorption of CV on the biochar was investigated

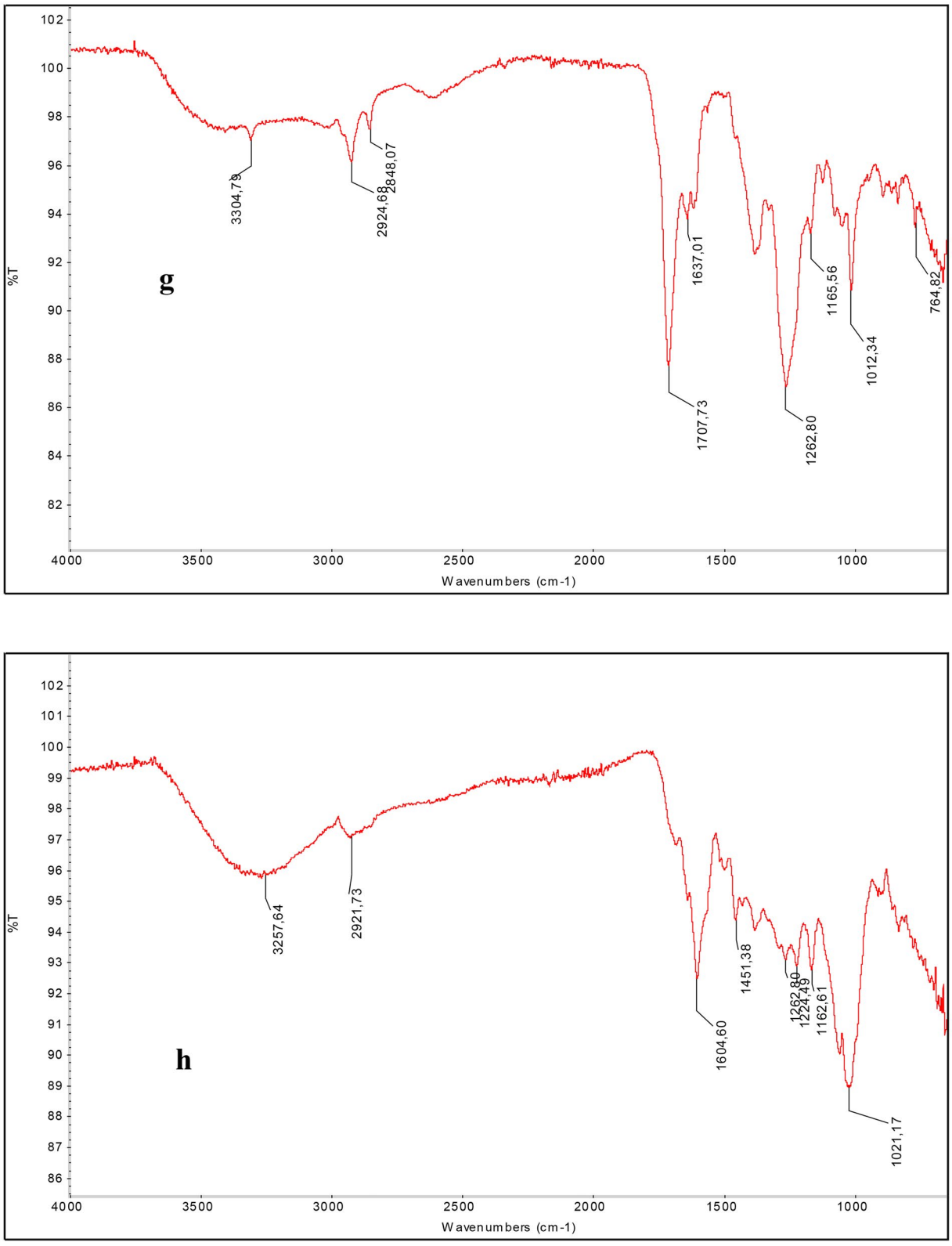


Figure 7. (g) *E. schimperi* biochar before adsorption and (h) *E. schimperi* biochar after adsorption.

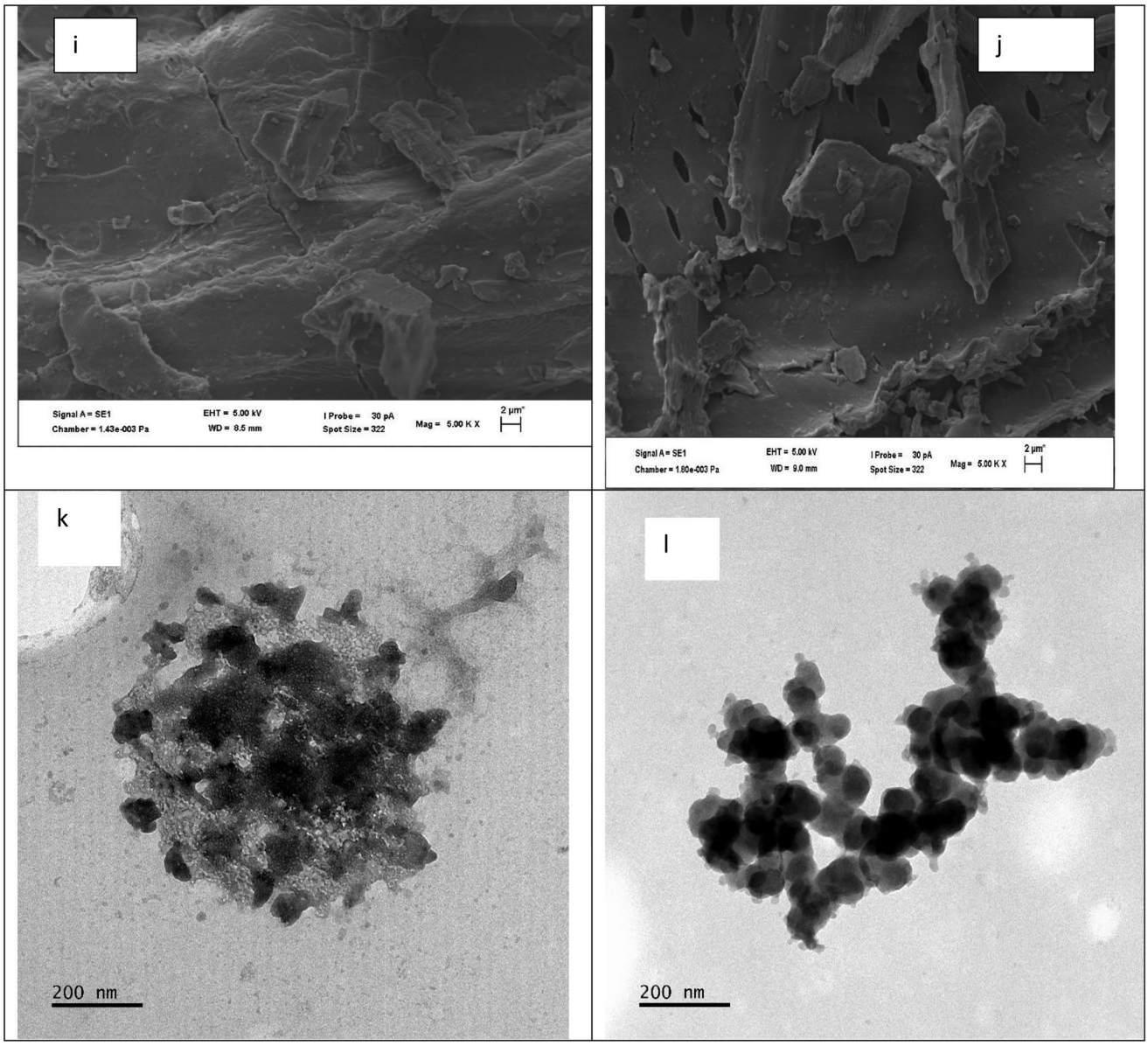


Figure 8. The SEM images of (i) before adsorption of CV and (j) after adsorption of CV; the TEM images of (k) before adsorption of CV B and (l) after adsorption of CV.

using classical and statistical methods for experimental design. Both studies show that adsorbent dosage, contact time, and pH significantly affect the percentage CV removal. From the predicted model generated by Minitab (ver. 17), the optimum removal was 98% at a 60 min optimum contact time, pH 7.5, and an adsorbent dose of 0.11 g.

Disclosure statement

No potential conflict of interest was reported by the author(s).

Funding

No funding was involved in this study.

Author contributions

CRediT: **Margaret Chepkemoi Koske**: Conceptualization, Formal analysis, Investigation, Methodology, Supervision, Validation, Writing – original draft, Writing – review & editing; **Michael David Otieno**: Conceptualization; **Ismael Okoth Oduor**: Formal analysis; **Charity Mutile Muendo**: Investigation.

ORCID

Margaret Chepkemoi Koske http://orcid.org/0000-0001-5481-1237

References

Aamir M et al. 2021. Graphene oxide nanocomposite with Co and Fe doped LaCrO3 perovskite active under solar light irradiation for the enhanced degradation of crystal violet dye. J Mol Liq. 322:114895. doi: 10.1016/j.molliq.2020.114895.

Ahmad W et al. 2021. Photocatalytic degradation of crystal violet dye under sunlight by chitosan-encapsulated ternary metal selenide microspheres. Environ Sci Pollut Res Int. 28(7):8074–8087. doi: 10.1007/s11356-020-10898-7.

Akdemir M, Isik B, Cakar F, Cankurtaran O. 2023. High-performing natural materials (Leonurus cardiaca): dye biosorption studies and

statistical analysis. Biomass Conv Bioref. 13(15):14281–14299. doi: 10.1007/s13399-023-04469-2.
Amin MT, Alazba AA, Shafiq M. 2021. Successful application of Eucalyptus camdulensis biochar in the batch adsorption of crystal violet and methylene blue dyes from aqueous solution. Sustainability. 13(7):3600. doi: 10.3390/su13073600.
Berk ME, Isik B, Ugraskan V, Cankurtaran O. 2025. Adsorptive removal of methylene blue dye onto sodium alginate/polythiophene composite microbeads: non-linear isotherm, kinetic, and thermodynamic study. Int J Biol Macromol. 316(Pt 2):144757. doi: 10.1016/j.ijbiomac.2025.144757.
Chahinez H-O, Abdelkader O, Leila Y, Tran HN. 2020. One-stage preparation of palm petiole-derived biochar: characterization and application for adsorption of crystal violet dye in water. Environ Technol Innov. 19:100872. doi: 10.1016/j.eti.2020.100872.
Cheng N et al. 2021. Adsorption of emerging contaminants from water and wastewater by modified biochar: a review. Environ Pollut. 273:116448. doi: 10.1016/j.envpol.2021.116448.
Chowdhary P, Bharagava RN, Mishra S, Khan N. 2020. Role of industries in water scarcity and its adverse effects on environment and human health. In: Environmental concerns and sustainable development. Springer. p. 235–256.
El Naeem GA et al. 2022. Adsorption of crystal violet and methylene blue dyes using a cellulose-based adsorbent from sugercane bagasse: characterization, kinetic and isotherm studies. J Mater Res Technol. 19:3241–3254. doi: 10.1016/j.jmrt.2022.06.045.
Essekri A et al. 2023. The use of raw and modified acacia leaves for adsorptive removal of crystal violet from water. Chem Eng Res Des. 190:143–156. 190:143-156. doi: 10.1016/j.cherd.2022.12.010.
Foroutan R, Peighambardoust SJ, Peighambardoust SH, Pateiro M, Lorenzo JM. 2021. Adsorption of crystal violet dye using activated carbon of lemon wood and activated carbon/Fe3O4 magnetic nanocomposite from aqueous solutions: a kinetic, equilibrium and thermodynamic study. Molecules. 26(8):2241. doi: 10.3390/molecules26082241.
Ganea I-V, Nan A, Baciu C, Turcu R. 2021. Effective removal of crystal violet dye using neoteric magnetic nanostructures based on functionalized poly (benzofuran-co-arylacetic acid): investigation of the adsorption behaviour and reusability. Nanomaterials (Basel). 11(3):679. doi: 10.3390/nano11030679.
Gurav R et al. 2021. Application of macroalgal biomass derived biochar and bioelectrochemical system with Shewanella for the adsorptive removal and biodegradation of toxic azo dye. Chemosphere. 264(Pt 2):128539. doi: 10.1016/j.chemosphere.2020.128539.
Homagai PL, Poudel R, Poudel S, Bhattarai A. 2022. Adsorption and removal of crystal violet dye from aqueous solution by modified rice husk. Heliyon. 8(4):e09261. doi: 10.1016/j.heliyon.2022.e09261.
Hu Z et al. 2019. Preparation of an antibacterial chitosan-coated biochar-nanosilver composite for drinking water purification. Carbohydr Polym. 219:290–297. doi: 10.1016/j.carbpol.2019.05.017.
Isik B, Cakar F, Cankurtaran O. 2023. Valorization of Urtica dioica roots as a highly-effective and eco-friendly biosorbent for adsorptive removal of hazardous textile dyes. Mater Sci Eng B. 293:116451. doi: 10.1016/j.mseb.2023.116451.
Khalil AT, Hameed S, Afridi S, Mohamed H, Shinwari ZK. 2021. Sageretia thea mediated biosynthesis of metal oxide nanoparticles for catalytic degradation of crystal violet dye. Mater Today Proc. 36:397–400. doi: 10.1016/j.matpr.2020.04.687.
Koske MC, Kiprop AK, Chepkwony SC, K'Owino I. 2022. Optimized dyeing of cotton with semi-synthetic embelin ninhydrin dye obtained by chemical modification of embelin from Embelia schimperi. J Nat Fibers. 19(16):13831–13839. doi: 10.1080/15440478.2022.2107143.
Kulkarni MR, Revanth T, Acharya A, Bhat P. 2017. Removal of crystal violet dye from aqueous solution using water hyacinth: equilibrium, kinetics and thermodynamics study. Resour Effic Technol. 3(1):71–77. doi: 10.1016/j.reffit.2017.01.009.
Kumar KV et al. 2019. Characterization of the adsorption site energies and heterogeneous surfaces of porous materials. J Mater Chem A. 7(17):10104–10137. doi: 10.1039/C9TA00287A.
Kumari S et al. 2025. Research hotspot and trend analysis of heavy metals decontamination of wastewater in past two decades: a bibliometric analysis. J Hazard Mater Adv. 17(2025):100532. doi: 10.1016/j.hazadv.2024.100532.
Kumari S, Singh R, Jahangeer J, Garg MC. 2024. Innovative strategies for dye removal from textile wastewater: a comprehensive review of treatment approaches and challenges. Water Air Soil Pollut. 235(11):720. doi: 10.1007/s11270-024-07532-4.
Li Z et al. 2020. Adsorption of congo red and methylene blue dyes on an ashitaba waste and a walnut shell-based activated carbon from aqueous solutions: experiments, characterization and physical interpretations. Chem Eng J. 388:124263. doi: 10.1016/j.cej.2020.124263.
Lin J, Xue C, Guo S, Owens G, Chen ZJC. 2021. Effects of green synthesized and commercial nZVI on crystal violet degradation by Burkholderia vietnamiensis C09V: dose-dependent toxicity and biocompatibility. Chemosphere. 279:130612. doi: 10.1016/j.chemosphere.2021.130612.
Lu M et al. 2023. Optimization of adsorption performance of cerium-loaded intercalated bentonite by CCD-RSM and GA-BPNN and its application in simultaneous removal of phosphorus and ammonia nitrogen. Chemosphere. 336:139241. doi: 10.1016/j.chemosphere.2023.139241.
Luyen NT, Linh HX, Huy TQ. 2020. Preparation of rice husk biochar-based magnetic nanocomposite for effective removal of crystal violet: Luyen, Linh, and Huy. J Elec Mater. 49(2):1142–1149. doi: 10.1007/s11664-019-07798-z.
Massoudinejad M, Rasoulzadeh H, Ghaderpoori M. 2019. Magnetic chitosan nanocomposite: fabrication, properties, and optimization for adsorptive removal of crystal violet from aqueous solutions. Carbohydr Polym. 206:844–853. doi: 10.1016/j.carbpol.2018.11.048.
Moharm AE et al. 2022. Fabrication and characterization of effective biochar biosorbent derived from agricultural waste to remove cationic dyes from wastewater. Polymers (Basel). 14(13):2587. doi: 10.3390/polym14132587.
Mustafanejad F, Sajjadi N, Marandi R, Zaeimdar M. 2021. Efficient removal of crystal violet by sulphonic-modified multi-walled carbon nano-tube and graphene oxide. Nanotechnol Environ Eng. 6(2):1–9. doi: 10.1007/s41204-021-00121-4.
Muthukumaran C, Sivakumar VM, Thirumarimurugan M. 2016. Adsorption isotherms and kinetic studies of crystal violet dye removal from aqueous solution using surfactant modified magnetic nanoadsorbent. J Taiwan Inst Chem Eng. 63:354–362. doi: 10.1016/j.jtice.2016.03.034.
Nono MM et al. 2025. Advances in adsorbent materials for heavy metals remediation: a roadmap for sustainability. Environ Monit Assess. 197(9):1016. doi: 10.1007/s10661-025-14289-8.
Omokpariola DO. 2021. Experimental modelling studies on the removal of crystal violet, methylene blue and malachite green dyes using Theobroma cacao (cocoa pod powder). J Chem Lett. 2:9–24. doi: 10.22034/jchemlett.2021.272842.1020.
Othmani A et al. 2021. Biochar and activated carbon derivatives of lignocellulosic fibers towards adsorptive removal of pollutants from aqueous systems: critical study and future insight. Sep Purif Technol. 274:119062. doi: 10.1016/j.seppur.2021.119062.
Palansooriya KN et al. 2020. Occurrence of contaminants in drinking water sources and the potential of biochar for water quality improvement: a review. Crit Rev Environ Sci Technol. 50(6):549–611. doi: 10.1080/10643389.2019.1629803.
Periyasamy AP. 2024. Recent advances in the remediation of textile-dye-containing wastewater: prioritizing human health and sustainable wastewater treatment. Sustainability. 16(2):495. doi: 10.3390/su16020495.
Qi X et al. 2021. Polydopamine/montmorillonite-embedded pullulan hydrogels as efficient adsorbents for removing crystal violet. J Hazard Mater. 402:123359. doi: 10.1016/j.jhazmat.2020.123359.
Radoor S et al. 2025. Adsorptive removal of crystal violet from aqueous solution by bioadsorbent. Biomass Conv Bioref. 15(2):2431–2442. doi: 10.1007/s13399-023-05079-8.
Rangabhashiyam S, Balasubramanian P. 2019. The potential of lignocellulosic biomass precursors for biochar production: performance, mechanism and wastewater application-a review. Ind Crops Prod. 128:405–423. doi: 10.1016/j.indcrop.2018.11.041.
Rehman F et al. 2018. Degradation of crystal violet dye by Fenton and photo-Fenton oxidation processes. Z Phys Chem. 232(12):1771–1786. doi: 10.1515/zpch-2017-1099.

Sackey EA, Song Y, Yu Y, Zhuang H. 2021. Biochars derived from bamboo and rice straw for sorption of basic red dyes. PLoS One. 16(7):e0254637. doi: 10.1371/journal.pone.0254637.

Samrot AV et al. 2021. Adsorption efficiency of chemically synthesized superparamagnetic iron oxide nanoparticles (SPIONs) on crystal violet dye. Curr Res Green Sustain Chem. 4:100066. doi: 10.1016/j.crgsc.2021.100066.

Sarabadan M, Bashiri H, Mousavi SM. 2019. Removal of crystal violet dye by an efficient and low cost adsorbent: modeling, kinetic, equilibrium and thermodynamic studies. Korean J Chem Eng. 36(10):1575–1586. doi: 10.1007/s11814-019-0356-1.

Sarioz N, Isik B, Cakar F, Cankurtaran O. 2024. Valorization of the performance of novel and natural sodium alginate/pectin/Portulaca oleracea L. ternary composites in the adsorption of toxic methylene blue dye from the aquatic environment. Int J Biol Macromol. 282(Pt 3):136867. doi: 10.1016/j.ijbiomac.2024.136867.

Sayed A et al. 2025. Unveiling the removal performance of banana peel biochar and rice husk nanoparticles for crystal violet and methylene blue dyes from aqueous media. Discov Environ. 3(1):143. doi: 10.1007/s44274-025-00354-z.

Pal J. 2024. Removal of lead ions from aqueous solution by modified nanocellulose. Environ Monit Assess. 196 (6):570. doi: 10.1007/s10661-024-12742-8.

Singh KP, Gupta S, Singh AK, Sinha S. 2011. Optimizing adsorption of crystal violet dye from water by magnetic nanocomposite using response surface modeling approach. J Hazard Mater. 186(2-3):1462–1473. doi: 10.1016/j.jhazmat.2010.12.032.

Soni S, Bajpai PK, Bharti D, Mittal J, Arora C. 2020. Removal of crystal violet from aqueous solution using iron based metal organic framework. Desalin Water Treat. 205:386–399. doi: 10.5004/dwt.2020.26387.

Srivatsav P et al. 2020. Biochar as an eco-friendly and economical adsorbent for the removal of colorants (dyes) from aqueous environment: a review. Water (Basel). 12(12):3561. doi: 10.3390/w12123561.

Tran HN, You S-J, Chao H-P. 2017. Insight into adsorption mechanism of cationic dye onto agricultural residues-derived hydrochars: negligible role of π-π interaction. Korean J Chem Eng. 34(6):1708–1720. doi: 10.1007/s11814-017-0056-7.

Tripathi A et al. 2022. ANN-GA based biosorption of As (III) from water through chemo-tailored and iron impregnated fungal biofilter system. Sci Rep. 12(1):12414. doi: 10.1038/s41598-022-14802-w.

van Rijn MH, Bech A, Bouyer J, van den Brand JA. 2017. Statistical significance versus clinical relevance. Nephrol Dial Transplant. 32(suppl_2):ii6–ii12. doi: 10.1093/ndt/gfw385.

Verma SP, Sarkar B. 2020. Analysis of flux decline during rhamnolipid based micellar-enhanced ultrafiltration for simultaneous removal of Cd+ 2 and crystal violet from aqueous solution. J Water Process Eng. 33:101048. doi: 10.1016/j.jwpe.2019.101048.

Vidya Vijay E, Jerold M, Sankar R, Lakshmanan S, Sivasubramanian V. 2019. Electrocoagulation using commercial grade aluminium electrode for the removal of crystal violet from aqueous solution. Water Sci Technol. 79(4):597–606. doi: 10.2166/wst.2019.066.

Vigneshwaran S, Sirajudheen P, Karthikeyan P, Meenakshi S. 2021. Fabrication of sulfur-doped biochar derived from tapioca peel waste with superior adsorption performance for the removal of Malachite green and Rhodamine B dyes. Surf Interfaces. 23:100920. doi: 10.1016/j.surfin.2020.100920.

Wang H et al. 2021. Effective adsorption of dyes on an activated carbon prepared from carboxymethyl cellulose: experiments, characterization and advanced modelling. Chem Eng J. 417:128116. doi: 10.1016/j.cej.2020.128116.

Zhang B, Wu Y, Cha L. 2020. Removal of methyl orange dye using activated biochar derived from pomelo peel wastes: performance, isotherm, and kinetic studies. J Disp Sci Technol. 41(1): 125-136 doi: 10.1080/01932691.2018.1561298.

Zhang J, Li F, Sun Q. 2018. Rapid and selective adsorption of cationic dyes by a unique metal-organic framework with decorated pore surface. Appl Surf Sci. 440:1219–1226. doi: 10.1016/j.apsusc.2018.01.258.